

## Antiferromagnetic ordering of Fe/Ru(0001)

Ruqian Wu

*Department of Physics and Astronomy, Northwestern University, Evanston, Illinois 60208-3112*

A. J. Freeman

*Department of Physics and Astronomy, Northwestern University, Evanston, Illinois 60208-3112  
and Material Science Division, Argonne National Laboratory, Argonne, Illinois 60439*

(Received 22 February 1991; revised manuscript received 2 May 1991)

The structural, electronic, and magnetic properties of the Fe/Ru(0001) system were determined by using the local-density total-energy full-potential linearized augmented-plane-wave energy-band method. Structurally, Fe atoms are found to occupy the hcp sites on the Ru(0001) substrate. Compared with the average of their bulk values, the nearest Fe-Ru distance contracts about 6% for the paramagnetic case but expands 1% for the ferromagnetic and the antiferromagnetic configurations, indicating the strong effect of magnetism and the lattice geometry. As the result of the strong overlayer-substrate hybridization, the Fe atoms, which are coupled ferromagnetically in the case of the corresponding free-standing Fe monolayer, favor antiferromagnetic coupling for Fe/Ru(0001). The predicted antiferromagnetic coupling appears to explain the observation by Liu and Bader that Fe overlayers on Ru(0001) are "magnetically dead" when the number of Fe layers is less than 2.

### I. INTRODUCTION

Recent technical progress makes it possible to synthesize high-quality ultrathin 3d transition-metal films. In turn, the observation of magnetic properties such as enhanced magnetic moments, perpendicular magnetic anisotropy, giant magnetoresistance, and lower-dimensional critical phenomena are stimulating fundamental studies, and are likely to open vast vistas for practical applications.<sup>1-2</sup>

Because of their technical and fundamental importance, ultrathin Fe films have received particularly close attention. Many experimental and theoretical works have been carried out to investigate the magnetic and electronic properties of, e.g., clean Fe surfaces, Fe overlayers on metal or ceramic substrates, and Fe superlattices with various kinds of interlayers, etc.<sup>3-9</sup> Qualitatively, Fe retains its ferromagnetism in most of the systems, although the value of the magnetic moment varies somewhat with details of the interaction with its surroundings. However, recent experimental results revealed unusual behavior in superlattice systems like Fe/Cr and Fe/Cu, where the ferromagnetic (FM) ultrathin Fe films couple antiferromagnetically via the magnetic or nonmagnetic intervening layers.<sup>10-13</sup> Among such systems, Fe/Ru is especially worthy of close attention because it was reported that the [Fe(111)]<sub>n</sub>/Ru(0001) overlayer system<sup>14</sup> and the hcp Fe<sub>n</sub>/15Ru<sub>m</sub><sup>15</sup> superlattice are "magnetically dead" when the number *n* of Fe layers is less than 2 (on the surface) or 4 (in the superlattice). Furthermore, as deduced from the thickness-dependent extrapolation, the ferromagnetism of the first 2 (4) Fe layers is not activated by deposition of successive FM Fe layers.

Four possibilities are proposed to explain these in-

teresting experimental observations for Fe/Ru systems.

(1) The strong Fe-Ru hybridization may entirely destroy the magnetism of the Fe layer since Fe atoms are paramagnetic (PM), i.e., magnetically dead, in Fe-Ru solid solutions when the concentration of Fe is less than 75%.<sup>15</sup> (2) For the same reason, interfacial interdiffusion, dislocations, etc., may also destroy the overlayer ferromagnetism. (3) Due to changes in the environment, the Fe atoms may couple in other more complicated ways, such as an antiferromagnetic (AFM) configuration. (4) Fe atoms may lose their magnetism in the hcp structure since the high-pressure  $\epsilon$ -Fe (hcp) is nonmagnetic.<sup>15</sup> The second possibility appears unlikely because not only is the surface-free energy of Ru higher than that of Fe, but it should influence the low-energy electron diffraction (LEED) pattern or destroy the perpendicular magnetic anisotropy.<sup>2</sup> In fact, as deduced from their Auger-intensity and LEED observations, Liu *et al.* reported a layer-by-layer growth mode for Fe/Ru(0001) at least for the first two Fe monolayers.<sup>14</sup> The fourth possibility should also be ruled out since the epitaxial growth enlarges the Fe-Fe interatomic distance (corresponding to a Wigner-Seitz radius  $R_{WS}$  of 2.7 a.u.); Podgóny *et al.*<sup>16</sup> reported, using linear-muffin-tin-orbitals-atomic-sphere-approximation (LMTO-ASA) approach, that the nonmagnetic-magnetic phase transition occurs when  $R_{WS} > 2.65$  a.u. ( $M = 2.4\mu_B$ ) for hcp Fe lattice. Furthermore, we found that a free-standing hexagonal Fe monolayer is ferromagnetic. Therefore, the observed "magnetically dead" phenomena should be attributed to interfacial effects only. The goal for theoretical work is thus to clarify whether the magnetism of the pseudomorphic Fe layers is entirely destroyed or whether merely the magnetic ordering is modified by the influence of the Ru substrate. In a recent LMTO-ASA calculation,

Knab *et al.*<sup>17</sup> found that the  $\text{Fe}_n/\text{Ru}_m$  superlattice is magnetically dead only when  $n = 1$ . For thicker Fe films, the antiferromagnetic coupling through the intervening Ru layers does become more favorable.

In this paper, the magnetic ordering and the electronic structure of Fe(111) as an overlayer on Ru(0001) is investigated by using the all-electron full-potential linearized augmented-plane-wave (FLAPW) total-energy method.<sup>18</sup> We found that in the in-plane AFM coupling is indeed the most stable magnetic configuration due to the strong Fe-Fu  $d$ -band hybridization, which explains the origin of the observed “magnetically dead layers.”<sup>14,15</sup> Furthermore, magnetic effects are very important in determining the overlayer relaxation for such a combined magnetic-nonmagnetic system. This “magnetic pressure” is especially pronounced when the magnetic moment depends sensitively on the interatomic spacing. In the following, the methodology and computational details are given in Sec. II, results and discussions, including the total energy analysis, magnetic moment and hyperfine field, valence charge density, and density of states, etc., are presented in Sec. III, and some conclusions are given in Sec. IV.

## II. METHODOLOGY AND COMPUTATIONAL DETAILS

The Fe/Ru(0001) system is simulated by a six-layer slab of an ideally constructed hcp Ru(0001) film covered by  $(1 \times 1)$  Fe(111) monolayers on each side. The 2D lattice constant and the distance between adjacent Ru planes are chosen from experiment ( $a = 5.114$  a.u.,  $c = 8.008$  a.u.),<sup>15</sup> while the location of Fe atoms and the overlayer relaxation are determined by total energy minimization. The overlayer FM and AFM couplings considered are sketched in Fig. 1, where the dashed lines show the smallest unit cell for each case. To simplify the calculations we obtain the structural properties by using the small cell [the rhombus in Fig. 1(a)] for FM and PM states. However, the supercell [the rectangle in Fig. 1(b)] is used to determine the AFM relaxation, and to examine part of the PM and FM results so as to minimize any systematic error.

As revealed by many Monte Carlo calculations based

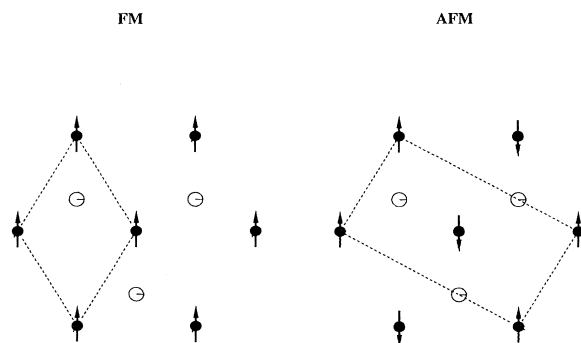


FIG. 1. Schematic ferromagnetic and antiferromagnetic overlayer configuration for Fe/Ru(0001). The dashed lines show the corresponding 2D unit cell.

on the 2D XY model, the AFM triangular magnetic lattice may exhibit very complicated configurations because of the inherent frustration.<sup>19,20</sup> The AFM configuration provided in this paper is only the simplest possibility but is not necessarily the lowest in total energy. To test the possible ground state proposed by Lee *et al.*<sup>20</sup> (with three sublattices forming  $\pm 120^\circ$  angles leading to a  $\sqrt{3} \times \sqrt{3}$  periodicity) requires a larger unit cell and lower spatial symmetry, and thus overwhelms the present computational ability.

In the FLAPW approach, no shape approximations are made to the charge densities, potentials, and matrix elements. The core states are treated fully relativistically and the valence states are treated semirelativistically (i.e., without spin-orbit coupling).<sup>21</sup> We employ the Hedin-Lundqvist and the von Barth-Hedin formulas for the exchange-correlation potentials for the nonmagnetic and the spin-polarized calculations, respectively.<sup>22</sup> About 500 augmented plane waves (APW's) for the small cell and 950 for the supercell (i.e., 60 APW's per atom) are used as a variational basis set, respectively. Within the muffin-tin (MT) spheres, lattice harmonics with angular-momentum  $l$  up to 8 are employed to expand the charge density, potential, and wave functions. Integrations over  $k$  space are substituted by summations over 18 (16) special  $k$  points in  $1/12$  ( $1/4$ ) irreducible 2D Brillouin zone (BZ) for the small cell (supercell).<sup>23</sup> Convergence is assumed when the average root-square distance between the input and output charge densities is less than  $5 \times 10^4 e/(\text{a.u.})^3$ . Consequently, total energy differences are reliable up to 1 mRy.

## III. RESULTS AND DISCUSSIONS

### A. Total energy analysis

As a first step we performed calculations for an fcc and an hcp stacked PM Fe overlayer to determine the structural ordering. We find that the total energy minimum for the fcc stacked overlayer is about 0.15 eV/atom higher than the corresponding value of the hcp one for the PM case. This energy difference is close to (or even larger for the FM case) the magnetic energy of 0.08~0.2 eV/atom. It is thus reasonable to assume that the energy ordering for these two kinds of stacking still holds for the spin polarized states, since the difference in the second neighbor interaction should not change the magnetic energy too much. In support of the assumption we should note that the spin polarization does not change the energy ordering between the fcc and the hcp overlayer stackings for both Co/Pt(111) and Co/Pd(111),<sup>24</sup> even though the magnetic energy is about four times larger than the energy difference for different locations for these two systems. Therefore, the Fe atoms occupy the hcp sites on the Ru(0001) substrate; we thus will not consider the fcc located overlayer in the results reported below.

Figure 2 presents the calculated total energy difference per Fe atom versus distance between the Fe and adjacent Ru atoms ( $d_{\text{Fe-Ru}}$ ) for the PM, FM and AFM hcp located Fe/Ru(0001). Obviously, the theoretical data can be well fitted by a parabola (solid lines) — indicating the

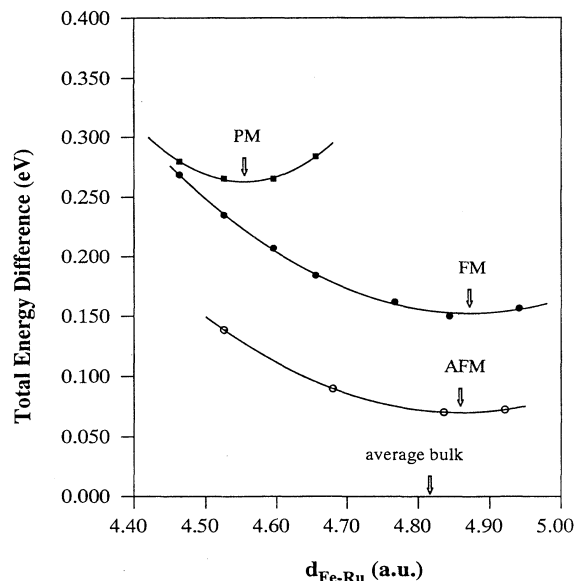


FIG. 2. Theoretical total energy difference per Fe atom of the hcp located Fe/Ru(0001) vs. the nearest Fe-Ru distance. The solid squares, solid and open circles represent the results for the PM, FM, and AFM states, respectively. Solid lines are the fitting parabolas. Arrows show the corresponding minimum positions.

precision of the total energies. The minimum in each fitted curve, pointed out by the arrows, gives the calculated equilibrium distances,  $d_{PM} = 4.55$  a.u. and  $d_{FM,AFM} = 4.85$  a.u. Compared to the unrelaxed Fe-Ru distance, 4.82 a.u. (defined as the average of the Fe-Fe and Ru-Ru bond lengths in their hcp bulk forms),<sup>15</sup> the PM Fe overlayer relaxes downwardly by 6%. Surprisingly, this large relaxation is entirely recovered by the magnetic polarization. As shown by the fitting curves for the FM and AFM states, the  $d_{Fe-Ru}$  even expands 1% compared to bulk average. This magnetically induced large expansion (7%), as revealed for many other systems,<sup>26</sup> suggests the strong effect of magnetism on the structural properties of Fe/Ru(0001).

Clearly, the total energy minima are found to order as AFM < FM < PM. The energy minimum of the AFM coupling is  $\sim 0.08$  eV per Fe atom lower than that for the FM case — indicating the stability of the AFM state. This result explains why the experimental observations by Liu and Bader<sup>14</sup> cannot detect ferromagnetism for Fe/Ru(0001). To derive the key factor (lattice strain or substrate effect) which leads to AFM ordering in the overlayer, a free-standing hexagonal Fe monolayer (ML) with an expanded 2D lattice constant (to match the Ru lattice) was also investigated. As a result the total energy for the FM state lies about 0.18 eV/atom (1.0 eV/atom) lower than that for the AFM (PM) state. Therefore, the AF coupling in the Fe overlayer originates entirely from the effect of the Ru(0001) substrate.

### B. Magnetism, spin polarization, and hyperfine field

The spatial distribution of the spin polarization, i.e., the spin densities, are presented in Figs. 3(a) and 3(b) on the vertical (11 $\bar{2}$ 0) plane for AFM and FM Fe/Ru(0001), respectively. Around the Fe atoms, the plots display evident spatial anisotropy (extend more into the vacuum), especially for the AFM state. The spin density decreases rapidly toward the interfacial direction and becomes negative around the adjacent Ru atoms. Therefore, the Ru(0001) substrate diminishes the overlayer magnetism. The overlayer magnetic perturbation in the interior of the substrate decays slowly (long-range effect), although the amplitude is small.

The theoretical magnetic moments inside each muffin-tin sphere ( $r_{MT} = 2.05$  a.u. for Fe,  $r_{MT} = 2.50$  a.u. for Ru) are listed in Table I for the FM and AFM Fe(111) ML's and for Fe/Ru(0001), respectively. For the FM Fe ML, we obtain an enhanced magnetic moment of  $2.90\mu_B$ , because of the expanded interatomic distance and lower coordination number (6). When it is deposited on the Ru(0001) substrate, the magnetic moment decreases drastically to  $2.24\mu_B$ . For the AFM state, the giant magnetic moment of  $2.87\mu_B$  for the Fe(111) ML is also reduced to  $2.23\mu_B$  for Fe/Ru(0001). Obviously, the effect of the overlayer-substrate hybridization diminishes the overlayer spin polarization substantially. This effect is more clearly seen by the strong dependence of the Fe magnetic moment,  $M$ , on  $d_{Fe-Fu}$  shown in Fig. 4. At small distances ( $d_{Fe-Ru} < 4.6$  a.u.), the FM moment is only  $\sim 1.3\mu_B$  — 40% smaller than that in the FM hcp or bcc Fe bulk ( $2.0, 2.2\mu_B$ )<sup>15</sup>. At intermediate distance

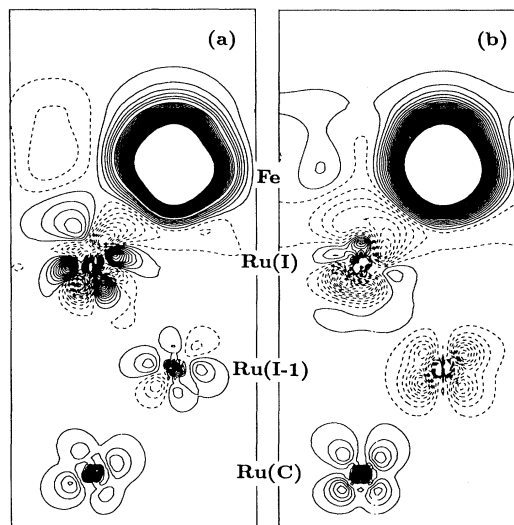


FIG. 3. The theoretical spin density of (a) AFM Fe/Ru(0001) and (b) FM Fe/Ru(0001). Contours shown on the vertical (11 $\bar{2}$ 0) plane start from  $\pm 5 \times 10^{-4}$  e/a.u.<sup>3</sup> and increase successively in steps of  $\pm 1 \times 10^{-3}$  e/a.u.<sup>3</sup>. The solid and dashed lines indicate positive and negative spin density, respectively.

TABLE I. The magnetic moment (in units of  $\mu_B$ ) for FM and AFM Fe ML's and Fe/Ru(0001).

System	Layer	FM	AFM
Fe ML	Fe	2.90	2.87
	Fe	2.24	2.23
Fe/Ru(0001)	Ru(I)	-0.08	-0.01
	Ru(I-1)	-0.08	0.6
	Ru(C)	0.04	0.05

4.6–4.8 (a.u.), the FM moment jumps by  $0.8\mu_B$  to  $2.2\mu_B$ , and shows a tendency to saturate thereafter. By comparison, the variation of the AFM moment with the  $d_{\text{Fe-Ru}}$  is smaller. It is enhanced by  $0.35\mu_B$  when  $d_{\text{Fe-Ru}}$  increases from 4.5 to 4.9 a.u. Since this kind of magnetic enhancement lowers the overlayer exchange energy (approaching the situation of the free-standing monolayer), it may somewhat compensate the overlayer-substrate chemical binding energy and thus is the chief factor driving the magnetically induced overlayer expansion.

The Fermi contact hyperfine field  $H_{CF}$ , which describes the coupling between the electronic spin and the nuclear magnetic moment, is proportional to the electronic spin density at the nucleus and is usually divided into contributions from core and valence electrons. As a well-established fact for magnetic transition metal bulks, surface, and overlayers, the core contribution (negative in sign) is proportional to the local magnetic moment.<sup>3,27</sup> The calculated  $H_{CF}$  at Fe nuclei for the FM and AFM Fe ML's and for Fe/Ru(0001) are presented in Table II. As expected, the core electron contribution is indeed proportional to the local magnetic moment; the ratio of the

TABLE II. Fermi-contact hyperfine field  $H_{CF}$  (in units of kG) for the FM and AFM Fe ML's and Fe/Ru(0001) broken down into valence and core contribution (given in units kG), the ratio of the core to magnetic moment  $M$  (in units of kG per  $\mu_B$ ).

	Fe ML		Fe/Ru(0001)	
	FM	AFM	FM	AFM
$H_{CF}$	-198	98	-214	-48
Valence	218	504	115	278
Core	-416	-406	-329	-328
Core/ $M$	-143	-142	-146	-146

core-hyperfine field and the magnetic moment for the FM and AFM Fe/Ru(0001) ( $146 \text{ kG}/\mu_B$ ) are identical even though their valence contributions are quite different. This ratio is also very close to the results for the Fe ML and moreover close to those obtained in other independent calculations.<sup>3,4,7,9</sup> By contrast, the valence (i.e., the conduction electron) contribution varies greatly for the different cases, as shown in Table II. Since the final  $H_{CF}$  values predicted also differ substantially ( $-214 \text{ kG}$  for the FM case,  $-48 \text{ kG}$  for the AFM case), one has a clear-cut means of confirming the predicted AFM ordering by means of conversion electron Mössbauer spectroscopy experiments.<sup>27-29</sup>

### C. Charge density and overlayer-substrate interaction

In Figs. 5(a) and 5(b), total charge density contours are shown on the vertical  $(11\bar{2}0)$  plane for AFM and FM Fe/Ru(0001), respectively. Because of the expanded Fe-Ru distance, the charge density in the region between the Fe and Ru atoms is slightly smaller than that in the region between adjacent Ru atoms. Unlike the spin density

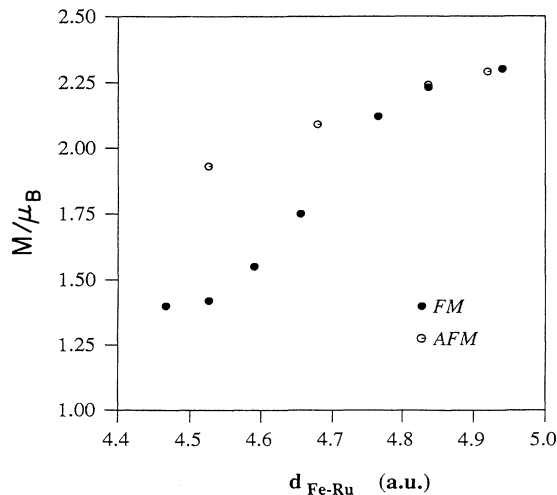


FIG. 4. The magnetic moment  $M$  of Fe/Ru(0001) vs. the nearest Fe-Ru distance. Solid and open circles represent results for the FM and AFM states, respectively.

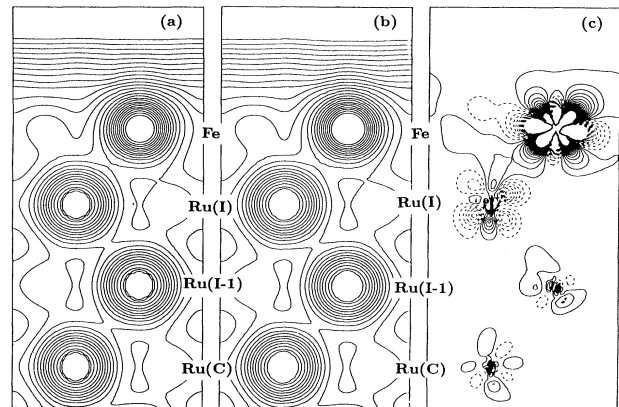


FIG. 5. The total valence charge density of (a) AFM Fe/Ru(0001), (b) FM Fe/Ru(0001), and (c) their difference ( $\rho_{\text{AFM}} - \rho_{\text{FM}}$ ) on the vertical  $(11\bar{2}0)$  plane. Contours in panels (a) and (b) start from  $5 \times 10^{-4} \text{ e/a.u.}^3$  and increase successively by a factor of  $\sqrt{2}$ . Contours in panel (c) start from  $\pm 2.5 \times 10^{-4} \text{ e/a.u.}^3$  and increase successively in steps of  $\pm 5 \times 10^{-4} \text{ e/a.u.}^3$ .

contours, the short-range metallic screening in the Ru(0001) substrate is evident, since the contours just under the interfacial Ru atoms are very similar to those around the center Ru atoms. This metallic screening effect is also reflected in Fig. 5(c) for  $\rho_{AFM} - \rho_{FM}$ , where the difference of the charge distribution is large around the interfacial Ru atoms but becomes very small in the interior region.

In order to reveal the physics of the overlayer-substrate interaction and its influence on the overlayer magnetism, the differences between the charge density of the Fe/Ru(0001) and the direct charge density superposition of the two corresponding Fe ML's and a clean Ru(0001) six-layer film are presented in Figs. 6 and 7 for the FM and AFM phases, respectively. In Fig. 6(a), strong bonding between the Fe and the interfacial Ru atom is obvious. Both Fe and Ru atoms lose electrons to the bonding region (covalent bonding). This bonding, as clearly shown by spin decomposition in Figs. 6(b) and 6(c), arises mainly from the minority spin states. For the majority spin states, aside from the fact that the Fe atoms lose electrons corresponding to the substrate induced decrease of the magnetic moment, a small contribution to the Fe—Ru bonding is also obvious. For the AFM case, as shown in Fig. 7, the overlayer-substrate bonding is even stronger for the total and the spin decompositions. The adsorption energy, which is defined as the total energy difference

$$E_{ad} = E_{Fe/Ru(0001)} - E_{Ru(0001)} - 2E_{Fe\ ML} \quad (1)$$

is 2.3 eV per Fe atom for the FM state and increases to 2.5 eV per Fe atom for the AFM case. The enhancement of the chemical bonding from AFM state to FM state is more clearly shown in Fig 5(c), where an excess occupa-

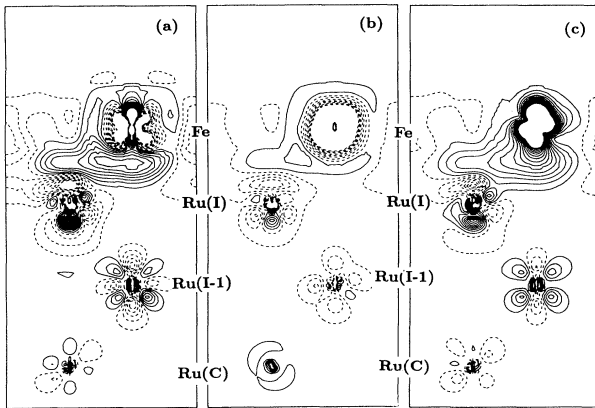


FIG. 6. Charge density difference between the FM Fe/Ru(0001) and the direct superposition of the free-standing FM Fe monolayer and the clean Ru(0001) surface for (a) total charge, (b) majority spin, and (c) minority spin. Contours on the vertical  $(11\bar{2})$  plane start from  $\pm 1 \times 10^{-3}$  e/a.u.<sup>3</sup> and increase successively in steps of  $\pm 2 \times 10^{-3}$  e/a.u.<sup>3</sup> Solid and dashed lines represent positive and negative differences, respectively.

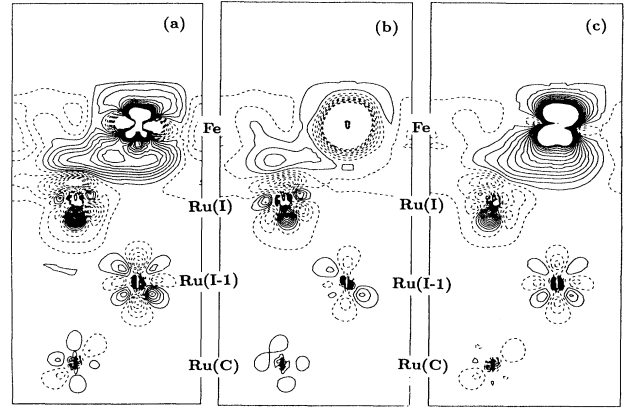


FIG. 7. Charge density difference between the AFM Fe/Ru(0001) and the direct superposition of the free-standing AFM Fe monolayer and the clean Ru(0001) surface for (a) total charge, (b) majority spin, and (c) minority spin. Contours on the vertical  $(11\bar{2})$  plane start from  $\pm 1 \times 10^{-3}$  e/a.u.<sup>3</sup> and increase successively in steps of  $\pm 2 \times 10^{-3}$  e/a.u.<sup>3</sup> Solid and dashed lines represent positive and negative differences, respectively.

tion of a  $d_{xz}$ -like state is apparent. The intrasublattice Fe-Fe interaction is also strengthened indirectly via the substrate for the AFM case whereas there exists a bond in the region just over the interfacial Ru atom in Fig. 5(c). These enhancements of the Fe-Fe and Fe-Ru interactions are responsible for the substrate induced stabilization of the AFV configuration.

#### D. Density of states analysis

The  $d$ -like density of states (DOS) projected in the Fe MT sphere for the FM and AFM Fe/Ru(0001), are plotted in Fig. 8 (solid lines), compared with the corresponding results for the Fe monolayer (dotted lines). For both FM and AFM Fe monolayers, the majority spin bands are almost fully occupied, and well separated from the minority spin bands (the exchange splitting is above 3 eV) — corresponding to the giant magnetic moment. Notice that the Fermi energy lies just at a peak of the AFM minority band, but is in the valley for the FM case. This may be the reason why the AFM phase is not stable for the free-standing Fe monolayer. For FM Fe/Ru(0001), due to the overlayer-substrate hybridization, the Fe  $d$  bands are significantly broadened. Both FM and AFM DOS curves extend in a wider energy range from  $-6$  eV to  $2$  eV — the entire energy range of the substrate  $d$  bands. The minority spin DOS at the Fermi energy decrease about two times from the value of the Fe monolayer for the AFM state but, by contrast, increase slightly for the FM case. This is of course helpful to stabilize the AFM state. As a result of the Fe-Ru interaction, majority (minority) spin bands lose (gain) some electronic occupation and, hence, the Fe magnetic moments are diminished. Compared to the FM case, states for AFM

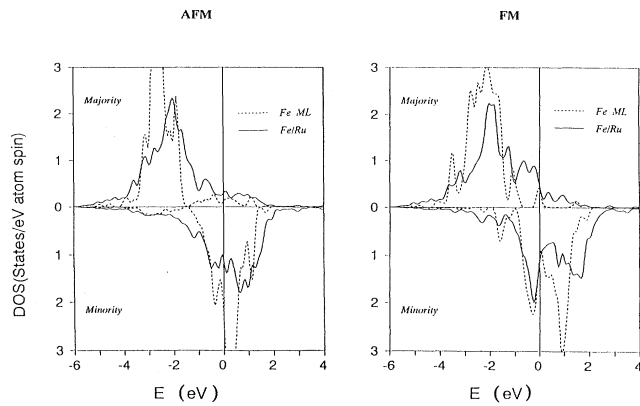


FIG. 8. The  $d$ -like density of states in Fe muffin-tin spheres for (a) AFM Fe monolayer (dashed) and AFM Fe/Ru(0001) (solid), (b) FM Fe monolayer (dashed) and FM Fe/Ru(0001) (solid). Energy scales are shifted with respect to the corresponding  $E_F$ , taken in each case as zero energy.

Fe/Ru(0001) lie in the lower energy region. As shown in Fig. 8, the majority spin peak between  $-1$  eV to the  $E_F$  for FM Fe/Ru(0001) is gone in the AFM DOS curve, while the AFM DOS is obviously larger at the  $d$  band bottom ( $-4$  eV to  $-2$  eV).

#### IV. CONCLUSION

The structural, electronic, and magnetic properties of the Fe/Ru(0001) system has been investigated by using precise FLAPW total energy calculations. We found that the in-plane AFM coupling becomes the stable ground state for Fe(111)/Ru(0001) due to strong Fe-Ru  $d$  band hybridization — which explains the origin of observed “magnetically dead layers.”<sup>14,15</sup> Strong Fe-Ru bonding results in a large adsorption energy of 2.4 eV per adatom and diminishes the overlayer magnetic moment. The Fe atoms occupy the hcp sites on the Ru(0001) substrate; the overlayer relaxes 6% for the PM state but expands 1% for the AFM and FM states. The pronounced “magnetic pressure” effect is attributed to the strong dependence of the local magnetic moment on the interatomic spacing for this system.

#### ACKNOWLEDGMENTS

We thank Dr. S. D. Bader, Dr. C. L. Fu, Dr. Chun Li, and Dr. C. Liu for helpful discussions. Work at Northwestern University was supported by the National Science Foundation [(Grant No. DMR88-16126) and by a grant of computer time at the Pittsburgh Supercomputing Center through its Division of Advanced Scientific Computing]. The work at Argonne National Laboratory was supported by the U. S. Department of Energy.

- <sup>1</sup>L. M. Falicov, D. T. Pierce, S. D. Bader, R. Gronsky, K. B. Hathaway, H. J. Hopster, D. N. Lambeth, S. P. Parkin, G. Prinz, M. Salamon, I. K. Schuller, and R. H. Victora, *J. Mater. Res.* **5**, 1299 (1990).
- <sup>2</sup>S. D. Bader, *Proc. IEEE* **78**, 909 (1990).
- <sup>3</sup>A. J. Freeman, C. L. Fu, S. Ohnishi, and M. Weinert, in *Polarized Electrons in Surface Physics*, edited by R. Feder (World Scientific, Singapore, 1986).
- <sup>4</sup>Chun Li, A. J. Freeman, and C. L. Fu, *J. Magn. Magn. Mater.* **75**, 201 (1988).
- <sup>5</sup>N. B. Brookes, A. Clarke, P. D. Johnson, and M. Weinert, *Phys. Rev. B* **41**, 2643 (1990).
- <sup>6</sup>C. Liu, E. R. Moog, and S. D. Bader, *J. Appl. Phys.* **64**, 5325 (1988).
- <sup>7</sup>C. L. Fu and A. J. Freeman, *Phys. Rev. B* **35**, 925 (1987).
- <sup>8</sup>J. Araya-Pochet, C. A. Ballentine, and J. L. Erskine, *Phys. Rev. B* **38**, 7846 (1988).
- <sup>9</sup>Chun Li and A. J. Freeman, *Phys. Rev. B* **43**, 780 (1991).
- <sup>10</sup>M. N. Baibich, J. M. Broto, A. Fert, F. Nguyen Van Dau, F. Petroff, P. Etienne, G. Creuzet, A. Friederich, and J. Chazelas, *Phys. Rev. Lett.* **61**, 2472 (1988).
- <sup>11</sup>G. Binasch, P. Grünberg, F. Sauerbach, and W. Zinn, *Phys. Rev. B* **39**, 4828 (1989).
- <sup>12</sup>S. S. P. Parkin, N. More, and K. P. Roche, *Phys. Rev. Lett.* **64**, 2304 (1990).
- <sup>13</sup>B. Heinrich, Z. Celinski, J. F. Cochran, W. B. Muir, J. Rudd, Q. M. Zhong, A. S. Arrott, and K. Myrtle, *Phys. Rev. Lett.* **64**, 673 (1990).
- <sup>14</sup>C. Liu and S. D. Bader, *Phys. Rev. B* **41**, 553 (1990).
- <sup>15</sup>M. Maurer, J. C. Ousset, M. Piecuch, M. F. Ravet and J. P. Sanchez, *Mat. Res. Soc. Symp. Proc. Vol. 151*, 99 (1989); M. Maurer, J. C. Ousset, M. Piecuch, and M. F. Ravet, *Europhys. Lett.* **9**, 803 (1989).
- <sup>16</sup>M. Podgóny and J. Goniakowski, *Phys. Rev. B* **42**, 6683 (1990).
- <sup>17</sup>D. Knab and C. Koenig, *Phys. Rev. B* **43**, 8370 (1991).
- <sup>18</sup>E. Wimmer, H. Krakauer, M. Weinert, and A. J. Freeman, *Phys. Rev. B* **24**, 864 (1981), and references cited therein.
- <sup>19</sup>S. Teitel and C. Jayaprakash, *Phys. Rev. B* **27**, 598 (1983).
- <sup>20</sup>D. H. Lee, J. D. Joannopoulos, J. W. Negele, and D. P. Landau, *Phys. Rev. Lett.* **52**, 433 (1984); *Phys. Rev. B* **33**, 450 (1986).
- <sup>21</sup>D. D. Koelling and B. N. Harmon, *J. Phys. C* **10**, 3107 (1977).
- <sup>22</sup>U. von Barth and L. Hedin, *J. Phys. C* **5**, 1629 (1972).
- <sup>23</sup>S. L. Cunningham, *Phys. Rev. B* **10**, 4988 (1974).
- <sup>24</sup>R. Wu, C. Li, and A. J. Freeman, *J. Magn. Magn. Mater.* (to be published).
- <sup>25</sup>J. F. Janak and A. R. Williams, *Phys. Rev. B* **14**, 4199 (1976).
- <sup>26</sup>K. B. Hathaway, H. J. F. Jansen, and A. J. Freeman, *Phys. Rev. B* **31**, 7603 (1985).
- <sup>27</sup>A. J. Freeman and R. E. Watson, in *Magnetism*, edited by G. T. Rado and H. Suhl (Academic, New York, 1965), Vol. IIA, p. 167.
- <sup>28</sup>J. Korecki and U. Gradman, *Phys. Rev. Lett.* **55**, 2491 (1985).
- <sup>29</sup>A. J. Freeman, C. L. Fu, M. Weinert and S. Ohnishi, *Hyperfine Interact.* **33**, 53 (1987).